Bright Retinal Lesions Detection using Colour Fundus Images Containing Reflective Features

L. Giancardo[1,2], E. Chaum[3], T.P. Karnowski[1], F. Meriaudeau[2], K.W. Tobin[1] and Y. Li[3]

[1] Oak Ridge National Laboratory, Oak Ridge TN, USA
[2] University of Burgundy, France
[3] Hamilton Eye Institute, U. Tennessee Health Sciences Center, Memphis TN USA

Abstract— **In the last years the research community has developed many techniques to detect and diagnose diabetic retinopathy with retinal fundus images. This is a necessary step for the implementation of a large scale screening effort in rural areas where ophthalmologists are not available. In the United States of America, the incidence of diabetes is worryingly increasing among the young population. Retina fundus images of patients younger than 20 years old present a high amount of reflection due to the Nerve Fibre Layer (NFL), the younger the patient the more these reflections are visible. To our knowledge we are not aware of algorithms able to explicitly deal with this type of reflection artefact.**

This paper presents a technique to detect bright lesions also in patients with a high degree of reflective NFL. First, the candidate bright lesions are detected using image equalization and relatively simple histogram analysis. Then, a classifier is trained using texture descriptor (Multi-scale Local Binary Patterns) and other features in order to remove the false positives in the lesion detection. Finally, the area of the lesions is used to diagnose diabetic retinopathy.

Our database consists of 33 images from a telemedicine network currently developed. When determining moderate to high diabetic retinopathy using the bright lesions detected the algorithm achieves a sensitivity of 100% at a specificity of 100% using hold-one-out testing.

Keywords— **computer-aided diagnosis, exudates, segmentation, LBP, NFL**

I. Introduction

The incidence of diabetes is constantly increasing, and with it related diseases such as diabetic retinopathy. Current studies show that the incidence of type 1 diabetes among young aged patients (0-19) in USA is one of the highest in the world and higher than all previously reported US studies and many European studies [1].

Non-mydriatic cameras connected to a telemedicine network are a possible solution to the rising number of diabetes patients and the shortage of ophthalmologists [2].

Exudates are a visible sign of diabetic retinopathy and a marker for the presence of retina edema. Various authors have developed segmentation algorithms for the automated detection of diabetic retinopathy [3, 4, 5], however to our knowledge none has explicitly addressed the problem of analysing a retina with a high degree of reflecting artefacts due to the nerve fibre layer (NFL). This structure is greatly visible in young patients especially on dark pigmented retinas like the one of African American patients as it is shown in Figure 1.

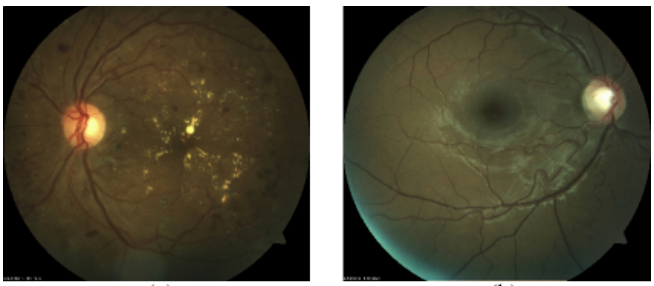

(a) (b)

Fig. 1: Fundus images showing exudates manifestations (a) and an healthy young retina with NFL reflectance (b).

We present an automatic diagnosis technique based on the segmentation of bright lesions that attempts to deal with this problem. We first describe our methodology, followed by preliminary results on a small database, finally the conclusions are presented.

II. Methodology

The algorithm presented is composed of three stages. In the first one, the colour retinal image undergoes an initial pre-processing stage to normalise the image by removing the mask and estimating the background. In the second stage, the analysis of the derivative of the global histograms of the red and green colour planes is used to produce an initial estimation of the bright lesion locations, which is refined employing a rough estimation of the vasculature and optic disc area. Then, a morphological close operation clusters together the neighbouring candidates. The clusters with an area of only a few pixels are removed. Various false positive lesions are identified at this stage. They are prominently caused by the

NFL reflection distant from the blood vessels. In the last part of the algorithm, we attempt to overcome this hurdle by training a LDA classifier to distinguish true from false lesions. The features used for the classification are based on a texture description of the different cluster of lesions as a whole, rather than pixel by pixel. This is accomplished by an adapted version of the Multicale Local Binary Pattern codes described by Menp and Pietikinen [6] and other simple statistical features. The images with suspected diabetic retinopathy are detected employing a simple threshold of the area of the lesions segmented in the final stage.

A. Stage I: Image Normalisation

The initial detection of the mask is particularly important for our algorithm, in fact many parameters are calculated based on the raw resolution of the image. Various cameras employ masks of different sizes and parameters will be inaccurate if the the ratio between mask and real retina size varies. The mask is extracted employing the green plane with 256 levels. A binary image containing all the pixels less than a threshold set to 10 levels more than the minimum value is created. A morphological close operation with disc shaped structuring element is performed to remove any watermark placed by the camera. The result is used to automatically maximise the effective area of the retina in the image obtaining I.

The majority of fundus images have backgrounds that vary across the image. This effect is partially due to illumination angles, partially due to the flash glare and also to the natural variation of the retina appearance. Foracchia at al. [7] devised a method to normalise contrast and illumination based on the identification of background pixels using a thresholded Mahalanobis distance in local windows. Grisan et al. [8] improved the previous technique by employing a mathematical model of the background illumination and noticing that contrast normalisation negatively affects lesion segmentation algorithms. In this system we employ the simpler technique of Niemeijer et al. [9]: the background image is produced by a median filter with a large window. We decided to use a square window of size:

$$medWin_1 = round(I_{width}/10) \tag{1}$$

where I_{width} is the width of the image I.

Informal experiments showed that even if the last method was not the one that provided the best background representation, it was able to highlight the lesions best with the process that is described in the next section. In fact, median filtering is general enough to take in account the natural change in the retinal appearance in addition to the luminosity changes.

B. Stage II: Lesion Candidate Segmentation

The background image I_{bg} is subtracted from the original image I on a channel by channel basis. The resulting image I_{sub} presents a peculiar histogram distribution that remains fairly constant throughout the various images, as can be seen in Figure 2.

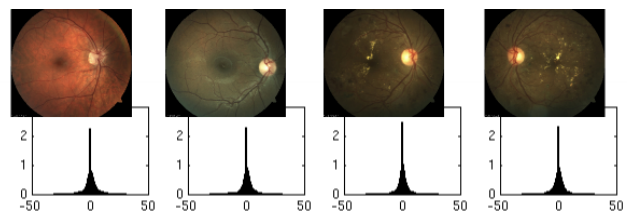

Fig. 2: Original images (top row) and histograms comparison of the green channels after the background normalisation (bottom row).

The positive side of the histogram contains: the optic nerve, bright lesions, NFL reflectance, other structures due to the natural variation of the retina and artefacts due to dirty lenses. On the other hand the negative side is characterised by: the vasculature, the macula, dark lesions and other structures due to the natural variation of the retina. With these premises a first selection of the bright lesion candidates is performed extracting all the pixels whose value is greater than T_{hist}, which is calculated as follows

$$\min_{T_{hist}} \sum_{T_{hist}=1}^{N} mod(d_{hist+}[T_{hist}]) < c_1 \tag{2}$$

where d_{hist+} is the quantised first derivative of the positive side of the I_{sub} histogram normalised by the number of pixels in the image. N is the number of bins in d_{hist+} and c_1 is an empirically derived constant equals to $5e-4$. This thresholding operation is performed on the green and red channels of I_{sub}. These channels are the ones appearing to have the clearest representation of the lesions. The binary images obtained are combined together using an AND operation obtaining I_{cand_1}.

A rough estimation of the vasculature is obtained from the analysis of the negative side of the histogram of I_{sub}. In this occasion only the green plane (I_{sub_g}) is used which seems to have the best representation of the vasculature. First, all the positive pixels in I_{sub_g} are set to 0, then a median filter of size $medWin_2 \, x \, medWin_2$ is used to remove the salt and pepper noise.

$$medWin_2 = round(I_{width} \cdot c_2) \tag{3}$$

where c_2 is equals to $48e-4$. The resulting image is binarised as follows:

$$I_{vess_1} = I_{sub_g_n} > 5 \tag{4}$$

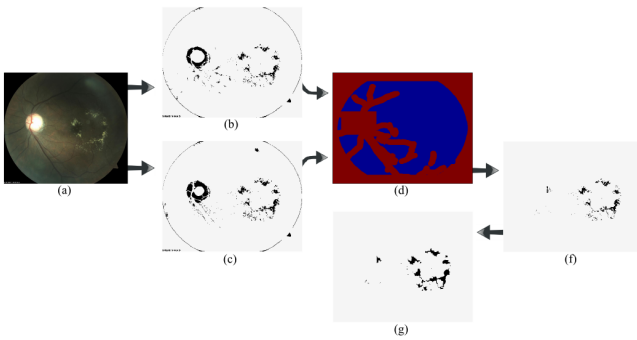

Fig. 3: Summary of the first two stages. (a) is the original I; (b) and (c) are respectively red and green of channels used to obtain I_{cand_1}; (d) shows the areas removed with the mask, ON and vasculature detection; (e) is I_{cand_2}; (f) is I_{cand_3}

where $I_{sub_g_n}$ is the previously denoised version of I_{sub_g}. I_{vess_1} contains an estimation of the vessels, the macula area and various small round retinal structures. In order to extract the vessels, a blob analysis is performed. Only the blobs with $circularity > 6$ are kept obtaining I_{vess_2}.

$$circularity = \frac{p^2}{4 \cdot \pi \cdot A} \tag{5}$$

where p is the perimeter and A is the area.

Much of the NFL reflectance is concentrated along the widest vessels. If small lesions were present in these areas they will not affect the sight because away from the macula. Because this paper attempts to recognise exudates typical of mild to high diabetic retinopathy, the area close to the vessels will not be evaluated for lesion candidates. This is accomplished by applying the Euclidean distance transform presented by Breu et al. [10] to I_{vess_2}, and removing all the lesions in I_{cand_1} with a distance from the vessels smaller than c_3 ($c_3 = I_{width} \cdot 0.02$).

The image obtained still contains various false positives that can be eliminated without relying on texture analysis, namely in the optic disk area and at the edges of the mask. The former can be identified using one of the optic disc (OD) detection techniques presented in the literature [11, 12], the latter by employing a dilated version of the mask retrieved in the first stage. The resulting image is referred as I_{cand_2}. In the current experiments the OD is removed with a simple method based on the detection of the highest mean luminosity value over local windows. This is suboptimal but seemed to work sufficiently well for the dataset used. The two final steps in the lesion candidate segmentation are: a morphological close operation with disc of size c_4 clusters the close lesion together and the removal of all the blobs with an area smaller than c_5 ($c_4 = I_{width} \cdot 71e-4$ and $c_5 = I_{width} \cdot 75e-4$). Figure 3 shows an example of the image obtained (referred as I_{cand_3}) and a summary of the first two lesion segmentation stages.

C. Stage III: Lesion Classification

This stage aims to distinguish true from false positive among the segmented lesions. The original image I is used, however the description of the retina textures is facilitated by substituting the vasculature and ON areas on I with the corresponding I_{bg}. This procedure attempts to hide foreground structures that might confuse the texture classification. For each cluster of lesions a 38 dimensional feature vector is generated. The first two dimensions contain the mean and the standard deviation of the red channel intensity in the area, the other 36 dimensions are occupied by histogram bins of Multiscale Local Binary Patterns (MLBP) of the blue channel.

The MLBP codes provide a compact way to describe textures invariant to rotation and illumination [6]. Four different scales are used with the parameters described in Table 1. The histogram of all the codes is calculated considering each scale as independent, then is normalised by the number of pixels in the cluster and added to the feature vector.

Table 1: MLBP parameters

Parameter	Scale 1	Scale 2	Scale 3	Scale 4
Gaussian filter support	6.7	15	33.7	75.5
LBP radius	4.8	10.8	24.3	54.6

A Fisher's linear discriminant classifier (LDA) is trained to distinguish true from false positives, by finding the hyperplane able to minimise the intra-class distance and to maximise the inter-class distance [13].

The training data is obtained by presenting each candidate lesion cluster to an expert who decides if it is a true positive, a false positive or if it is not a good example of either category and it should be left out the training process.

The referral to ophthalmologist decision is taken based on the area of the true lesions detected. Mild to High diabetic retinopathy is diagnosed when the area occupied by lesions is greater than the 0.5% of the total area of the image.

III. Results

The dataset employed consisted of 33 anonymised images from a telemedicine study in Memphis, Tennessee [2]. They are grabbed by a VisuCam Pro NM, a commercial non-mydriatic fundus camera produced by Zeiss. The images manifest a considerable degree of NFL reflectance, as shown on a scale from 0 to 4 in Table 2. All but two come from African American patients. 29 images present an healthy

retina and 4 a mild to high diabetic retinopathy condition. The conditions of patients and NFL information are determined by one of the co-authour Dr. E. Chaum, a qualified ophthalmologist.

Table 2: NFL reflectance distribution in the dataset

	NFL 0	NFL 1	NFL 2	NFL 3	NFL 4
Number of Images	2	17	10	2	2

The tests are performed on the entire dataset using hold-one-out technique. Table 3 summarises the results of the lesion segmentation and the suggested diagnosis using different colour planes to calculate the MLBP codes. It can be noticed that the diagnosis sensitivity and specificity do not vary using different features set. However, the best lesion segmentation performance was obtained using the Blue channel which presents the fewest false positives occurrence with the most true positive as it can be inferred by the lesion areas found in the healthy and DR retinas.

Table 3: Diagnosis results using different colour planes to derive the MLBP codes. The first four rows are a statistical measures of the area of the lesions segmented expressed as percentage of the total effective image area. The last two rows contain the diagnosis information.

	Red MLBP	Green MLBP	Blue MLBP
Healthy Retina mean of lesion area	0.017%	0.015%	0.009%
Healthy Retina std of lesion area	0.017%	0.015%	0.009%
DR retina mean of lesion area	0.017%	0.015%	0.009%
DR retina std of lesion area	0.017%	0.015%	0.009%
Diagnosis - Sensitivity	100%	100%	100%
Diagnosis - Specificity	100%	100%	100%

The total computation burden to normalise, segment and classify a 1024x1024 image is $\sim$23 seconds obtained with an unoptimised MATLAB implementation on a 1.6 GHz machine with 4 GB of RAM.

IV. Conclusions

A new technique to aid the screening process for diabetic retinopathy in patients with high degree of NFL reflections has been presented. Although the dataset used to validate the algorithm is very small, we feel that we have demonstrated its ability to diagnose patients with exudates even in presence of artefacts created by reflective features.

Future work will concentrate on validating this method on larger databases containing images showing all diabetic retinopathy stratifications.

Acknowledgements

This work was supported in part by the National Eye Institute of the National Institutes of Health (R01-EY017065). This paper was prepared by the OAK RIDGE NATIONAL LABORATORY, Oak Ridge, Tennessee, USA, 37831-6285, operated by UT-BATTELLE, LLC for the US DEPARTMENT OF ENERGY under contract DE-AC05-00OR22725.

References

1. Bell Ronny A, Mayer-Davis Elizabeth J, Beyer Jennifer W, et al. Diabetes in non-Hispanic white youth: prevalence, incidence, and clinical characteristics: the SEARCH for Diabetes in Youth Study. *Diabetes Care.* 2009;32 Suppl 2:S102–S111.
2. Chaum Edward, Karnowski Thomas P, Govindasamy V. Priya, Abdelrahman Mohamed, Tobin Kenneth W. Automated diagnosis of retinopathy by content-based image retrieval. *Retina.* 2008;28:1463–1477.
3. Osareh A., Mirmehdi M., Thomas B., Markham R.. Automated identification of diabetic retinal exudates in digital colour images. *Br J Ophthalmol.* 2003;87:1220–1223.
4. Garca Mara, Snchez Clara I, Lpez Mara I, Absolo Daniel, Hornero Roberto. Neural network based detection of hard exudates in retinal images. *Comput Methods Programs Biomed.* 2009;93:9–19.
5. Niemeijer Meindert, Ginneken Bram, Russell Stephen R, Suttorp-Schulten Maria S A, Abrmoff Michael D. Automated detection and differentiation of drusen, exudates, and cotton-wool spots in digital color fundus photographs for diabetic retinopathy diagnosis. *Invest Ophthalmol Vis Sci.* 2007;48:2260–2267.
6. Menp Topi, Pietikinen Matti. Multi-scale Binary Patterns for Texture Analysis in *Image Analysis, 13th Scandinavian Conference* 2003.
7. Foracchia Marco, Grisan Enrico, Ruggeri Alfredo. Luminosity and contrast normalization in retinal images. *Med Image Anal.* 2005;9:179–190.
8. Grisan E., Grisan E., Giani A., Ceseracciu E., Ruggeri A.. Model-based illumination correction in retinal images in *Proc. 3rd IEEE International Symposium on Biomedical Imaging: Nano to Macro* (Giani A.. , ed.):984–987 2006.
9. Niemeijer M., Ginneken B., Staal J., Suttorp-Schulten M. S. A., Abramoff M. D.. Automatic detection of red lesions in digital color fundus photographs 2005;24:584–592.
10. Breu H., Gil J., Kirkpatrick D., Werman M.. Linear time Euclidean distance transform algorithms 1995;17:529–533.
11. Karnowski Thomas P, Govindasamy V. Priya, Tobin Kenneth W, Chaum Edward. Locating the optic nerve in retinal images: comparing model-based and Bayesian decision methods. *Conf Proc IEEE Eng Med Biol Soc.* 2006;1:4436–4439.
12. Abramoff M.D., Niemeijer M.. The automatic detection of the optic disc location in retinal images using optic disc location regression in *Proc. 28th Annual International Conference of the IEEE Engineering in Medicine and Biology Society EMBS '06*:4432–4435 2006.
13. Duda RO, Hart PE, Stork DG. *Pattern Classification*. Wiley-Interscience 2001.